Photoproduction of the π^0 meson off protons from 2.775 to 5.45 GeV

M. C. Kunkel* and M. J. Amaryan
Old Dominion University, VA (U.S.A.)

I. Strakovsky
The George Washington University, Washington, DC (U.S.A.)

(and the CLAS Collaboration)

(Dated: September 23, 2016)

Exclusive neutral pion photoproduction ($\gamma p \to p\pi^0$) was measured in the CLAS detector at the Thomas Jefferson National Facility. The experiment employed a 1.1-5.5 GeV bremsstrahlung photon beam from 5.6 GeV electron beam created in the Continuous Electron Beam Accelerator Facility (CEBAF). The photon beam energy was impinged on a liquid hydrogen target. The neutral pions were detected via external conversion, $\pi^0 \to \gamma\gamma \to e^+e^-\gamma$, and subsequent Dalitz decay, $\pi^0 \to \gamma^*\gamma \to e^+e^-\gamma$. Measured differential cross-sections, $\frac{d\sigma}{dt}$ and $\frac{d\sigma}{d\cos\theta}$ are compared with the constituent counting rule, Regge and handbag theoretical calculations. The results for the constituent counting rule agree well with the data. The Regge theoretical calculations underestimate the differential cross sections between 3.9 and 4.6 GeV, but agree with data at photon energies 4.6-5.4 GeV. The handbag theoretical calculation significantly underestimates the data at center of mass energies, s $\sim$ 11 GeV.

I. INTRODUCTION

In hadron physics, photoproduction of single pion is essential to understand the photon-nucleon vertex. At low energies, the photon-nucleon coupling establishes excited nucleon resonances which has been at the forefront of physics "missing resonances" search. At high energies single pion photoproduction can be used to test predictions of Regge theory, in which recent calculations [1] have shown to describe the presented data well. Furthermore, these measurements have shown that the differential cross section for single pion photoproduction at fixed c.m. angles, $\theta_{c.m.}$, of 70°, 90° and 110° seem to scale as $\frac{d\sigma}{dt} \sim s^{2-n} f(\theta_{c.m.})$, where s and t are the Mandelstam variables and n is the total number of interacting elementary fields in the initial and final state of the reaction. This is predicted by the constituent counting rule [2, 3] and exclusive measurements in pp and $\bar{p}p$ elastic scattering [4, 5], meson-baryon Mp reactions [5], and photoproduction γN [6–13] agree well with this rule. The following paper details the CLAS g12 experiment, the extraction of single neutral pion photoproduction from data, the differential cross-sections through the entire beam energy range of the g12 experiment, a comparison of the differential cross-section with existing world data, as well as the comparison of the data to the model given in [1] and a comparison to the constituent counting rule.

II. EXPERIMENTAL SETUP

The measurements used for this analysis was taken with the `CLAS` detector at Hall B at the Thomas Jefferson National Accelerator Facility `TJNAF` located in Newport News, Virginia. The *g12* experiment is a photoproduction experiment, it ran during March - June 2008 with a total of 44 days of good beam time. It collected over 128 TB of raw data that consisted of $26 \cdot 10^9$ events, with an integrated luminosity of 68 pb^{-1}. The photon beam was produced by impinging a 5.715 GeV electron beam, at 65nA, on a Au radiator of 10^{-4} radiation length. Photons in the energy range from 20% to 95% of the electron beam energy were tagged, resulting in a photon beam energy range of 1.1-5.5 GeV. This photon beam was then collimated before being introduced onto a ℓH_2 target 40 cm in length along the z-direction and 2 cm radius. The placement of the target was 90 cm upstream from `CLAS` center (toward Au radiator), this increased the acceptance of particles in the forward direction. During the runtime of *g12*, the Cherenkov detectors were filled with perfluorobutane (C_4F_{10}) allowing for electron/positron detection. The experiment had a dedicated trigger, amongst 9 other triggers, that consisted of Cherenkov Counter(`CC`) and Electro-magnetic Calorimeter(`EC`) coincidence hits for the entire beam energy range. With proper cuts on the `CC` and `EC` a π/e rejection of 10^6 for $e^\pm$ pairs was established.

III. EVENT SELECTION

Pions were skimmed initially and then re-identified as leptons by changing the mass of the pion. This method is sufficient when the decaying particle's mass, i.e. m_{π^0},

* Now at Forschungszentrum Jülich; m.kunkel@fz-juelich.de

is less than that of $\pi^{\pm}$. If the event satisfied the requirements listed in Table I, then all timing, momentum and vertex information was outputted as well as CC and EC information to be used to identify leptons, as discussed in Sec IV. To reduce the size of the data set, a cut was placed on the total missing mass of $\gamma p \to p\pi^+\pi^-$ to be less than 275 MeV. This cut was broad enough to not interfere with π^0 selection from single π^0 production i.e. $\gamma p \to p\pi^0$ when assigned the pion the lighter mass of a electron/positron. This broad cut also does not interfere with π^0 production from light meson decay, i.e $\gamma p \to p\omega \to p\pi^+\pi^-\pi^0$.

TABLE I. Requirements of initial skim

Requirement
One in-time beam photon
One proton
One π^+ or *"unknown"* of q^+
One π^- or *"unknown"* of q^-

IV. PARTICLE IDENTIFICATION

Lepton identification was based on conservation of mass. Once the data is skimmed according to Table I, all particles that were π^+, π^-, unknown with q^+ or unknown with q^- were tentatively assigned to be electrons or positrons based on their charge.

A. Kinematic Cuts

First it should be noted that for the /g12 experiment, there was a two-prong trigger for events in which the photon beam energy was greater then 3.6 GeV, while for the entire data taking process there was a "lepton" trigger configuration. Therefore to measure the differential cross-section at photon beam energies less than 3.6 GeV this "lepton" trigger information was employed. Once particle section was achieved, it was necessary to reduce the background of the exclusive $\gamma p \to p\pi^+\pi^-$ reaction. For events of photon beam energy less than 3.6 GeV, a CC and EC "hit" must have been recorded for each charge track that was not the proton. For all events 3 kinematic fits were performed, a 1-C ($\gamma p \to pe^+e^-(\gamma)$) to identify the missing photon in the reaction, a 4-C ($\gamma p \to p\pi^+\pi^-$) as a discriminator and a 2-C ($\gamma p \to p\pi^0 \to pe^+e^-(\gamma)$) to identify the reaction. After the kinematic fit, a 1% confidence level cut was placed on the 1-C fit. The missing energy of the $\gamma p \to pe^+e^-$ spectrum versus the missing mass of $\gamma p \to pX$ was analyzed and shown that a 75 MeV cut on the missing energy was suitable to suppress the $\gamma p \to p\pi^+\pi^-$ reaction. After the missing energy cut, the signal to background ratio was $\sim$ 99.7%, see right figure 1, the other 4-C and 2-C fits were then used with a 1% confidence on each to suppress the background to $\sim$ 99.9%.

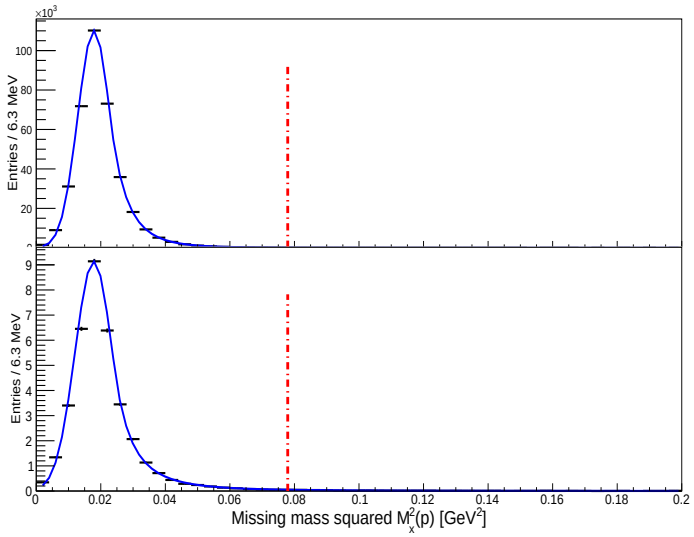

FIG. 1. (Black points)$M_x^2(p)$ data used in analysis. (Blue line) Fit using Crystal Ball function. The horizontal red dashed-dotted line depicts the threshold of $\pi^+\pi^-$ production. Top:Data for photon energies below 3.6 GeV. Bottom:Data for beam photon energies greater than 3.6 GeV

V. MONTE-CARLO

There are certain kinematic regions of CLAS in which physics events are not being recorded properly i.e. the area dividing each sector in CLAS. Furthermore each sector in CLAS is asymmetric in the acceptance of events due to subsystem inefficiencies such as inoperable Drift Chamber(DC) wires, photomultiplier(PMT) inefficiencies, dead scintillator strips in the Time-of-Flight(TOF) and Start Counter(ST) subsystems. When a triggered event is recorded and reconstructed these asymmetric inefficiencies factors are reflected and must be carefully understood because these factors are properties of the CLAS detector and independent of any physics that occurred. To properly understand the detector effects on the data, CLAS utilizes a GEANT3 simulation package know as GSIM. The acceptance for the cross-sections presented in this work was measured using phase-space Monte-Carlo (MC) simulation, using PLUTO++ [14] as the generator, for the reaction channels,

$$\begin{aligned} \gamma \mathrm{p} &\to p\pi^0 \\ &\hookrightarrow p\gamma\gamma \\ &\hookrightarrow pe^+e^-\gamma \end{aligned} \tag{1a}$$

$$\begin{aligned} \gamma \mathrm{p} &\to p\pi^0 \\ &\hookrightarrow pe^+e^-\gamma. \end{aligned} \tag{1b}$$

A total of events, N_g, was generated and this number was weighted by the relative branching ratios found in [32] to resemble the conditions of the data. The number of events generated for the reaction channel 1a can be found in Table II as N_c. The number of events generated for the reaction channel 1b can be found in Table II as N_d. After the events are generated, they are inputted into the

TABLE II. Number of generated events in each decay spectrum

Quantity	Value·10^7	Description
N_g	240	π^0 events generated
N_c	237	$\pi^0 \to \gamma\gamma$ events generated
N_d	2.8	$\pi^0 \to e^+e^-\gamma$ generated

CLAS simulation chain and then reconstructed with the same program used to reconstruct the data. Once the events are reconstructed, the cuts described in Sec. IV A are applied. The acceptance $\eta(E_\gamma, \theta^{\pi^0}_{C.M.})$ is then determined by adding the simulations for the conversion and the dalitz, then for photon energy bins of 25 MeV increments and $\Delta\cos\theta^{\pi^0}_{C.M.} = 0.0125$ increments, the ratio of reconstructed events (N_R) to generated events (N_G) yields,

$$\eta(E_\gamma, \cos\theta^{\pi^0}_{C.M.}) = \frac{N_R(E_\gamma, \cos\theta^{\pi^0}_{C.M.})}{N_G(E_\gamma, \cos\theta^{\pi^0}_{C.M.})} \ . \tag{2}$$

The $\Delta\cos\theta^{\pi^0}_{C.M.}$ binning in the acceptance is a factor of 2.4 finer than the smallest $\Delta\cos\theta^{\pi^0}_{C.M.}$ increment used in the cross-section measurement.

VI. SYSTEMATIC UNCERTAINTIES

Systematic errors are caused the controls of the experiment, such as flux, simulation, density and length of the ℓH_2 target and also systematic errors are caused by various analytical tools used, such as the kinematic fitter.

A. Branching Ratio Systematic Uncertainty

The branching ratios for the two topologies used to measure the cross-section were obtained from [32] and are listed again in Table III with their associated errors. Uncorrelated quantities that are summed as,

$$f = \sum_{i=1}^{M} a_i P_i \tag{3}$$

have errors as

$$\sigma_f = \sqrt{\sum_{i=1}^{M} (a_i\sigma_i)^2}. \tag{4}$$

Therefore

$$\frac{\Gamma}{\Gamma_{tot}} = \frac{\Gamma_{\pi^0\to e^+e^-\gamma}}{\Gamma_{tot}} + \frac{\Gamma_{\pi^0\to\gamma\gamma\to e^+e^-\gamma}}{\Gamma_{tot}} \tag{5}$$

$$= \frac{\Gamma_{\pi^0\to e^+e^-\gamma}}{\Gamma_{tot}} + \frac{\Gamma_{\pi^0\to\gamma\gamma}P(\gamma\to e^+e^-)}{\Gamma_{tot}} \ , \tag{6}$$

where $P(\gamma \to e^+e^-)$ is the probability of photon conversion into e^+e^-. To measure $P(\gamma \to e^+e^-)$, the acceptance for conversion ($P(\gamma \to e^+e^-)\cdot\eta_{e^+e^-}$) is divided by the acceptance for Dalitz ($\eta_{e^+e^-}$). The conversion probability depends on incident photon energy. A maximum probability of 8% per-photon was measured. Therefore,

$$\frac{\Gamma}{\Gamma_{tot}} = \frac{\Gamma_{\pi^0\to e^+e^-\gamma}}{\Gamma_{tot}} + \frac{\Gamma_{\pi^0\to\gamma\gamma}P(\gamma\to e^+e^-)}{\Gamma_{tot}} = 0.09 \ , \tag{7}$$

and has error

$$\sigma_f = \sqrt{\left(\frac{1}{\Gamma_{tot}}\right)^2 (\sigma^2_{\pi^0\to e^+e^-\gamma} + \sigma^2_{\pi^0\to\gamma\gamma})} = 0.0037. \tag{8}$$

The energy and $\cos\theta$ dependence of the conversion is accounted for in the acceptance, which is E_γ and $\cos\theta$ bin-dependent.

TABLE III. Branching ratio and errors used in $\frac{d\sigma}{d\cos\theta^{\pi^0}_{C.M.}\, d\phi}$ measurements

Quantity	Value	Error
$\Gamma_{\pi^0\to\gamma\gamma}$	0.98823	0.00034
$\Gamma_{\pi^0\to e^+e^-\gamma}$	0.01174	0.00035
$\frac{\Gamma}{\Gamma_{tot}}$	0.13	0.0037

B. Cut Based Systematic Uncertainty

The procedure to determine the systematic uncertainty of the cuts placed on the various kinematic fits was first to calculate an acceptance with a different cut, then to calculate a new total cross-section measurement applying the different cut to the data. The total cross-section was computed at various photon beam energies. Lets denote the original measured total cross-section as Ξ_1 and the new total cross-section determined by the new cut as Ξ_n, then the systematic error was calculated as.

$$\sigma_{cut} = \frac{|\Xi_1 - \Xi_n|}{\Xi_1} \tag{9}$$

Some systematic uncertainty depended on the photon energy. All cut based systematics were performed individually, meaning when a cut was changed, the remaining cuts retained their original value, see Table IV for the values of the cuts that were changed to calculate the systematic error.

TABLE IV. Different Cuts to analyze systematics

Cut	Original	Adjusted	Uncertainty
2-C Fit	1%	10%	0.0219
1-C Fit	1%	10%	$0.00216+0.01083E_\gamma$
4-C Fit	1%	10%	0.00031
Missing Energy	75 MeV	100 MeV	0.02781

C. Photon Flux Systematic Uncertainty

The photon flux calculation should be consistent throughout the experiment. If the flux measurement is not consistent due to corrections made with the live-time, beam corrections or fractional difference in the reported current to the actual current during the photon flux normalization run then a systematic uncertainty would be produced. It was deduced that for the entire *g12* run, the lower limit for the flux normalization uncertainty was 6%.

D. Detector Efficiency Systematic Uncertainty

Each sector in `CLAS` can be treated as an individual detector, with its own efficiency and resolution. A systematic uncertainty could arise if one or more of the sectors is not simulated properly. It was determined that this systematic uncertainty was incident beam energy dependent.

E. z-vertex Cut Systematic Uncertainty

The systematic uncertainty of the z-vertex cut was analyzed by varying the initial vertex cut from $-110 \leq z \leq -70$ to $-109 \leq z \leq -71$ for both data and `MC`. Afterward the procedure for determining the systematic was identical to the method used to determine the "Cut Based Systematic Uncertainty". The systematic uncertainty from varying the z was 0.0041.

F. Target Systematic Uncertainty

Since the systematic on the density is 0.02% the maximum systematic on the target is due to uncertainty in the length on the target which is 40 cm ± 0.2 cm. A total systematic on the target was assign to be 0.5%.

G. Total Systematic Uncertainty

The total systematic uncertainty along with a list of the individual systematics is presented in this subsection. The calculation of the total systematic error is

$$\sigma_{tot}^{sys} = \sqrt{\sum_{i=1}^{M} \sigma_i^2} \tag{10}$$

For the data presented in this manuscript the lowest systematic uncertainty, at $E_\gamma = 2.775$ GeV, is 9.72%, while the highest systamtic uncertainty, at $E_\gamma = 5.425$ GeV, is 11.9%.

TABLE V. Systematic errors used in $\frac{d\sigma}{d\cos\theta^{\pi^0}_{C.M.}\, d\phi}$ measurements

Systematic	Error
Sector	$0.0361 + 0.0065E_\gamma$
Flux	0.06
Missing Energy Cut	0.02781
2-C Fit Pull Probability	0.0219
1-C Fit Pull Probability	$0.00216 + 0.01083E_\gamma$
4-C Fit Pull Probability	0.00031
Target	0.005
Branching Ratio	0.0037
Fiducial Cut	0.024
z-vertex Cut	0.0041
Total	$\sqrt{(5.7 + 0.52E_\gamma + 0.16E_\gamma^2) \cdot 10^{-3}}$

VII. COMPARISON WITH THEORETICAL MODELS

There are several models that attempt to describe π^0 photoproduction in the low beam energy resonance region, while in the high beam energy regime there exists limited amount of theory. Described below are two theories.

1. *HandBag Model*

The production of the π^0 meson in photon-proton reactions, for incoming photon beam energies greater than 2.8 GeV, can considered to be a hard exclusive reaction. One approach to study the π^0 photoproduction, is use the handbag model. In the handbag approach, the reaction is factorized into two parts. The first part is when one quark from the incoming and one from the outgoing nucleon participate in the hard sub-process. This hard sub-process is achieved when the incident photon excites a quark, since quarks are bound quantum particles, the excited quark produces a jet of quarks that form the meson and then de-excites back into the nucleon. This is calculable using pQCD. The second part ,the soft part, consists of all the other quarks that are spectators and can be described in terms of GPDs [15–18]. The handbag

mechanism is applicable when the Mandelstam variables, s, t, u, are large as compared to a hadronic scale of order 1 GeV . In Ref. [19] a model, derived from the handbag approach, has been applied to predict angular dependence of scaled photoproduction cross section of π^0 and is illustrated in Fig. 2. The handbag model calculations by Kroll *et al.* [19] does not agree with the measurement obtained by *g12*.

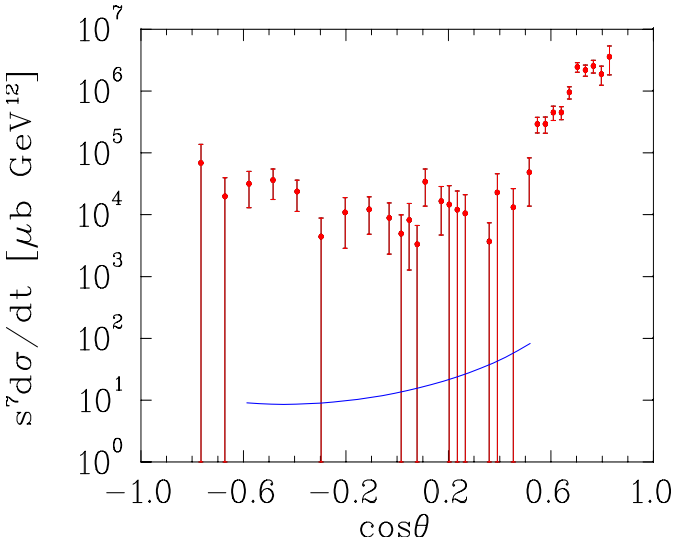

FIG. 2. Comparison of the π^0 differential cross section photoproduction data to GDP handbag model. Experimental data at $s = 11.08$ GeV^2 are from the current (red filled circles). The theoretical prediction at $s = 10$ GeV^2 by [19] is given by blue solid line.

A. Constituent Counting Rule

The constituent counting rule (CCR) predicts the energy dependence of the differential cross-section at fixed center-of-mass angles for an exclusive two-body reactions. It validity is at high beam energies and large momentum transfer and the framework is similar to that of the handbag approach, in which the theory relies on the factorization of the exclusive process into a hard scattering amplitude and a soft quark amplitude inside the hadron. The prediction of CCR is:

$$\frac{d\sigma}{dt} \sim s^{2-n} f(\theta_{c.m.}) \tag{11}$$

where s and t are the Mandelstam variables, n is the total number of interacting elementary fields in the initial and final state of the reaction and $f(\theta_{c.m.})$ depends on the dynamics of the process. Many exclusive measurements in pp and $\bar{p}p$ elastic scattering [4, 5], meson-baryon Mp reactions [5], and photoproduction γN [6–13] agree well with this rule. For π^0 photoproduction reactions CCR predicts that the differential cross-section $\frac{d\sigma}{dt}$ should scale as s^{-7}, where -7 was calculated from 4 elementary fields in the initial state, 1 for the photon, 3 for the number of quarks in a proton, and 5 elementary fields in the final state, 3 quarks from the proton and 2 quarks from the π^0 , 2-9 =-7. A comparison of this previous data along with the *g12* measurements can be seen in figure 3, at high energies and large angles the results are consistent with the s^7 scaling expected from the quark counting rule.

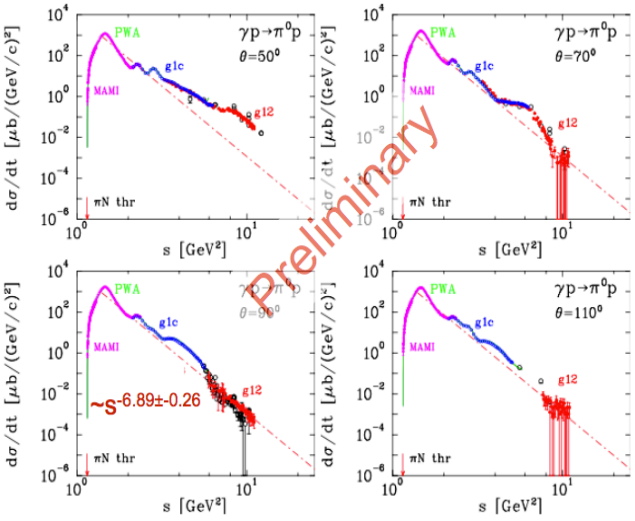

FIG. 3. The differential cross section for the $\gamma p \to p\pi^0$ reaction at $\theta_{c.m.} = 50°, 70°, 90°, 110°$, as a function of s (center of mass energy squared). Experimental data are from the current measurement (red filled circles), CLAS [20, 21] (blue circles), MAMI [22] (magenta circles), old measurements [23] (black open circle plus). The dash dotted line is a result of the fit performed at $\theta = 90°$ with power function $\sim s^n$ leading to n = 6.89 ± 0.26.

[1] V. Mathieu *et al.*, Phys. Rev. **D92**, p. 074013 (2015), arXiv:1505.02321 [hep-ph].

[2] S. J. Brodsky and G. R. Farrar, Phys. Rev. Lett. **31**, 1153–1156 (1973).

[3] G. P. Lepage and S. J. Brodsky, Phys. Rev. D **22**, 2157–2198 (1980).

[4] P. Landshoff and J. Polkinghorne, Physics Letters B **44**, 293 – 295 (1973).

[5] R. L. Anderson *et al.*, Phys. Rev. D **49** (1994).

[6] W. Chen *et al.* (The CLAS Collaboration), Phys. Rev. Lett. **103**, p. 012301 (2009).

[7] L. Y. Zhu *et al.* (Jefferson Lab Hall A Collaboration), Phys. Rev. Lett. **91**, p. 022003 (2003).

[8] R. A. Schumacher and M. M. Sargsian, Phys. Rev. C **83** (2011).

[9] R. L. Anderson *et al.*, Phys. Rev. D **14**, 679–697 (1976).

[10] J. Napolitano *et al.*, Phys. Rev. Lett. **61**, 2530–2533 (1988).

[11] J. E. Belz *et al.*, Phys. Rev. Lett. **74**, 646–649 (1995).

[12] C. Bochna *et al.*, Phys. Rev. Lett. **81**, 4576–4579 (1998).

[13] E. C. Schulte and others., Phys. Rev. Lett. **87** (2001).

[14] I. Frohlich, I. Froehlich, L. Cazon, T. Galatyuk, V. Hejny, *et al.*, PoS **ACAT2007**, p. 076 (2007), arXiv:0708.2382 [nucl-ex].

[15] X.-D. Ji, Phys.Rev.Lett. **78**, 610–613 (1997).

[16] X. Ji, Phys. Rev. D **55**, 7114–7125 (1997).

[17] A. Radyushkin, Phys.Lett. **B380**, 417–425 (1996).

[18] M. Diehl, T. Feldmann, R. Jakob, and P. Kroll, Eur.Phys.J. **C8**, 409–434 (1999).

[19] H. W. Huang and P. Kroll, Eur.Phys.J. **C17**, 423–435 (2000).

[20] M. Dugger *et al.*, Phys.Rev. **C76**, p. 025211 (2007), 0705.0816.

[21] M. Dugger *et al.* (CLAS Collaboration), Phys.Rev. **C88**, p. 065203 (2013), 1308.4028.

[22] R. Beck, Eur. Phys. J. A, **28**, 173–183 (2006).

[23] P. Joss, Compilation of photoproduction data above 1.2 gev, 1970.

[24] O. Bartholomy *et al.* (CB-ELSA Collaboration), Phys.Rev.Lett. **94**, p. 012003 (2005), hep-ex/0407022.

[25] V. Crede *et al.* (CBELSA/TAPS Collaboration), Phys.Rev. **C84**, p. 055203 (2011), 1107.2151.

[26] A. Anisovich *et al.*, Eur.Phys.J. **A44**, 203–220 (2010), 0911.5277.

[27] M. Sumihama *et al.*, Phys.Lett. **B657**, 32–37 (2007), 0708.1600.

[28] O. Bartalini *et al.* (GRAAL Collaboration), Eur.Phys.J. **A26**, 399–419 (2005).

[29] M. Braunschweig *et al.*, Physics Letters B **26**, 405 – 409 (1968).

[30] W. Briscoe *et al.*, Institute of Nuclear Studies of The George Washington University Database,.

[31] M. Fuchs *et al.*, Physics Letters B **368**, 20 – 25 (1996).

[32] K. O. et al (Particle Data Group), Phys. Rev. C **38**, p. 090001 (2014).